

# Reliability Computation of Piezoelectric Actuator Embedded in Flexible Smart Rectangle Cantilever Beam under Complex Gust Load

Yongfeng Fang,<sup>1\*</sup> Zizhe Fang,<sup>2</sup> Kong Fah Tee,<sup>3,4</sup> and Yaofei Tuo<sup>5</sup>

<sup>1</sup>Department of Electrical Engineering and Automation, School of Physics and Electric Information Engineering, Ningxia Normal University, Yanzhou, Guyuan 756000, China

<sup>2</sup>Department of Mechanical Engineering, School of Mechanical Engineering and Automation, Northeastern University, Shenyang 110819, China

<sup>3</sup>Department of Civil and Environmental Engineering, King Fahd University of Petroleum and Minerals, Dhahran 31261, Saudi Arabia

<sup>4</sup>Interdisciplinary Research Center for Construction and Building Materials, KFUPM, Dhahran 31261, Saudi Arabia

<sup>5</sup>Department of Mechanical, School of Energy Engineering, Yulin University, Yuyang, Yulin 719000, China

(Received February 2, 2023; accepted April 26, 2023)

**Keywords:** gust, piezoelectric sensor and actuator, flexible cantilever beam, reliability

Piezoelectric sensors and actuators have been widely used in many fields. In this study, the reliability of a piezoelectric actuator to alleviate the flutter of a flexible rectangular cantilever beam under wind load is investigated. Firstly, a dynamic calculation model of the cantilever beam underload is derived. Secondly, the derived dynamic calculation model of the cantilever beam is extended with a piezoelectric actuator. Thirdly, two types of wind load on the beam are considered. Finally, the reliability of using one and two actuators to alleviate the flutter of the beam under different wind loads is simulated. The proposed calculation model has practical engineering significance and feasibility for the reliability design and maintenance of unmanned aerial vehicle (UAV) wings and wind power devices.

## 1. Introduction

The flexible rectangle cantilever beam (FRCB), owing to its lightweight, large span, and large deformation, is widely used in unmanned aerial vehicles (UAVs) and wind power, micromachinery, and many other applications. However, the FRCB can easily flutter under load because of its low strength and stiffness, thus affecting the overall stability and operation efficiency of equipment.<sup>(1)</sup> In recent years, piezoelectric actuators, which are made of piezoelectric materials, have often been used in the wings of UAVs to alleviate, for example, the flutter and drive micromachines, which showed good effects.<sup>(2,3)</sup> A smart piezoelectric cantilever beam is often used to fabricate self-powered vibration sensors. The equation of the output voltage of a smart piezoelectric cantilever beam under vibration has been established and its output voltage analyzed.<sup>(4)</sup> A highly flexible multifunctional wing with embedded piezoelectric

---

\*Corresponding author: e-mail: [fangyf\\_9707@126.com](mailto:fangyf_9707@126.com)  
<https://doi.org/10.18494/SAM4345>

materials for adaptive vibration control was studied,<sup>(5)</sup> and the active control algorithms for the gust alleviation of the piezoelectric device functions were obtained. The optimal design method of a flexible mechanism and the driving signal of a stick-slip piezoelectric actuator were studied. A stick-slip piezoelectric actuator prototype with an optimized flexible mechanism was manufactured. It was shown that the mechanism of an optimized flexible piezoelectric actuator could be provided by two factors, the force and the rectified driving signal. Moreover, the operating velocity of the piezoelectric actuator could be enhanced by 20.56 and 29.48% at 100 and 1000 Hz, respectively.<sup>(6)</sup>

To solve the problem of elastic vibration of a flexible spinning missile, a method of applying a piezoelectric stack actuator to the control of elastic vibration was proposed.<sup>(7)</sup> The flexible spinning missile was simplified to a nonuniform free–free Timoshenko beam model, considering the gyro effect and thrust, the piezoelectric stack actuator was applied to the control of the elastic vibration of the missile, and the dynamic model of the flexible spinning missile with the piezoelectric stack actuator was established on the basis of the finite element method.<sup>(8)</sup> The fabrication and characterization of flexible cantilevers based on aluminum nitride (AlN) as a piezoelectric active layer and polyimide as an elastic substrate were studied.<sup>(9)</sup> By using the residual compressive stress of polyimide multilayer material, a flexible cantilever beam with a piezoelectric layer was successfully fabricated by a double-mask process.

The mechanical response of the realized flexible cantilevers has been investigated by piezoresponse measurements, and the experimentally obtained first resonance frequency was around 15 kHz. Reliability is an important index because it is used as a measure of whether a smart structure can fulfill a given function at a given time. The computation and evaluation of reliability are essential in scientific and engineering analyses. For all smart structures, reliability should be considered and studied.<sup>(10,11)</sup> On the basis of the finite element method, a simple roughness model consisting of semicircles of constant radius along the surface of an RF-MEMS switch is employed. This model can be used to compute the reliability of the shifts in electromechanical characteristics of RF-MEMS switches due to surface roughness.<sup>(12)</sup>

A method of evaluating the reliability of the electromechanical actuators on aircraft was developed, the algorithm of which is based on the reconstruction of the residual torque in mechanical transmissions.<sup>(13)</sup> It is shown that friction magnet and permanent magnet are the most suitable permanent magnet motors with good torque density, reliability, and high speed. Furthermore, on the basis of the characteristics of permanent magnets, the integration of the torque limiter within the actuator motor was investigated. Such integration can lead to improved reliability as well as higher power density.<sup>(14)</sup> An electrical model of an induction machine is coupled with a lumped parameter model of a two-stage gear system to build an integrated model of these systems. The mechanical and electrical outputs of the piezoelectric cantilever beam under the inverse piezoelectric condition were studied. The limit state equation for the mechanical and electrical reliabilities of the piezoelectric cantilever beam under the inverse piezoelectric effect has been derived, and it has been shown that the proposed model is robust and practical with validation by an engineering problem.<sup>(15)</sup> The reliability of the cantilever beam with interval parameters was calculated by using the first-order second-moment method.<sup>(16)</sup> Antoniadis *et al.* proposed a novel dynamical adaptive enhanced simulation method

coupled with support vector regression. The method is shown to be highly applicable to solving engineering problems with complex nonlinear performance functions.<sup>(17)</sup> Reliability provides information on the relative importance of model input quantities and the information support optimization as well as model checking.

To ensure the reliability and safety of smart piezoelectric structures during the service period, it is necessary to calculate, analyze, and evaluate the reliability of flexible smart piezoelectric structures. Studies about the reliability of flexible smart piezoelectric structures are limited. Over ten years, our team has been studying piezoelectric sensors and actuators, during which, the reliability of the piezoelectric sensors and actuators was computed, and the output force of the actuators was analyzed. On the basis of the above literature, in this study, the reliability of a flexible piezoelectric smart rectangle cantilever beam (FPSRCB) is investigated under complex wind loads. Firstly, the dynamic calculation model of the flexible rectangle cantilever beam under load is derived. Secondly, the dynamic calculation model of the FPSRCB is proposed. Thirdly, the calculation based on two wind load styles on the cantilever beam is considered. Finally, the reliabilities of the FPSRCBs with one and two actuators under different wind loads are simulated. The reliability calculation method used in this study has practical engineering significance and feasible applications to the reliability design and maintenance of UAV wings, wind turbine devices, micromachines, and others.

## 2. Kinetic Analysis of FRCB

If it is equipped without the piezoelectric actuator, the FRCB can be assumed as a Euler–Bernoulli beam as shown in Figs. 1(a) and 1(b). Figure 1(a) shows a photograph of the FRCB, which is a part of the front wing of a UAV, and Fig. 1(b) is a schematic of the FRCB.

When the FRCB is subjected to multiple loads, two types of deformation occur: bending and twisting. The equation of motion of the FRCB with these two types of deformation is

$$E = E_b + E_t, \quad (1)$$

where  $E_b$  is the kinetic energy associated with the bending moment of the beam as it bends downward and  $E_t$  is the kinetic energy associated with torsion when the FRCB is twisted.

It is assumed that the FRCB conforms to the bending moment and torsion generation conditions of the Euler–Bernoulli beam. The kinetic energy associated with the bending movement can be described as

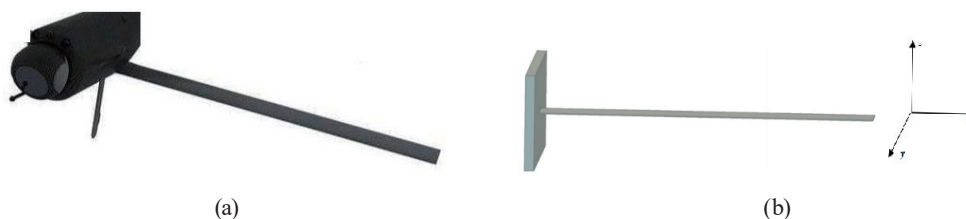


Fig. 1. (a) Photograph and (b) schematic of FRCB, a UAV component.

$$E_b = \frac{1}{2} \int_{\Omega} \rho \left[ \left( -z \frac{\partial w}{\partial y} \right)^2 + \left( \frac{\partial w}{\partial z} \frac{dz}{dt} + \frac{\partial w}{\partial y} \frac{dy}{dt} \right)^2 \right] d\Omega, \tag{2}$$

where  $\rho$  is the density of the material of the FRCB,  $\Omega$  is the spatial domain integrated and encompasses the elastic structure, and  $w$  is the bending moment deformation. The kinetic energy associated with the torsion movement can be described as

$$E_t = \frac{1}{2} \int_{\Omega} \rho (x^2 + z^2) \left( \frac{\partial \alpha}{\partial x} \frac{dx}{dt} + \frac{\partial \alpha}{\partial y} \frac{dy}{dt} + \frac{\partial \alpha}{\partial z} \frac{dz}{dt} \right)^2 d\Omega, \tag{3}$$

where  $\alpha$  is the torsion angle.

### 3. Mechanical and Electrical Analyses of FPSRCB

The flowchart of the FPSRCB using excitation power to alleviate the flutter of the FRCB is shown in Fig. 2.

The FPSRCB contains embedded piezoelectric actuators and sensors as shown in Fig. 3. The FPSRCB showed flutter because of the airflow and wind load during its service period. The feedback information on the amplitude and frequency of the flutter is sent to the control center by the piezoelectric sensors. The voltage used to stimulate the piezoelectric actuators is released by the control center according to the feedback information. The piezoelectric actuators are deformed repeatedly, the FPSRCB is vibrated because of the piezoelectric actuators, and the amplitude of the flutter will be alleviated.

The FPSRCB can be assumed as a mechanic-electric coupling system, and its dynamic equation is<sup>(6)</sup>

$$\Pi = \frac{1}{2} \int_{\Omega} \sigma \varepsilon d\Omega - \frac{1}{2} \int_{\Omega} D \Xi d\Omega + \frac{1}{2} \int_{\Omega} I J_{\alpha} \left( \frac{\partial \alpha}{\partial y} \right)^2 d\Omega, \tag{4}$$

where  $\sigma$  is the mechanical stress,  $D$  is the electrical displacement,  $\Xi$  is the electric field,  $I$  is the shear modulus,  $J_{\alpha}$  is the torsion constant of the cross section, and  $\varepsilon$  is the mechanical strain associated with bending described as

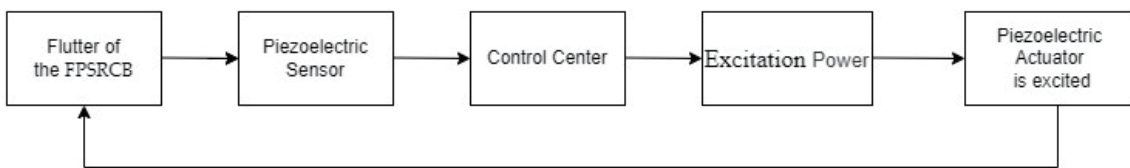


Fig. 2. Flowchart of FPSRCB using excitation power to alleviate the flutter of FRCB.

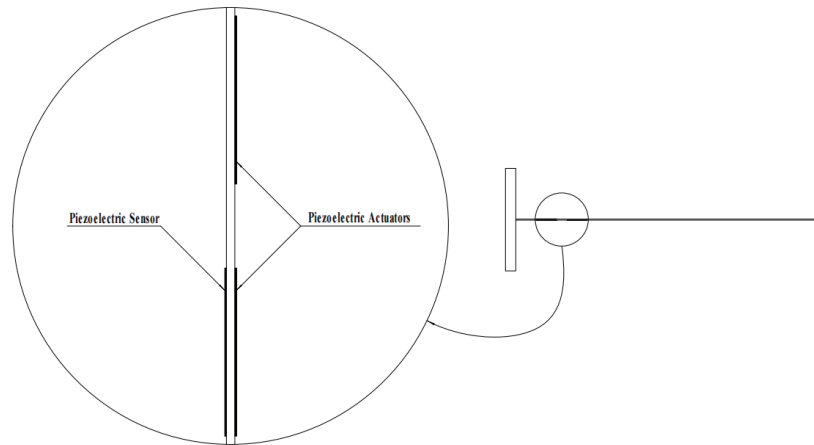


Fig. 3. FPSRCB.

$$\varepsilon = -zw_{,yy} \tag{5}$$

Once the constitutive relations of linear piezoelectric actuators are defined by

$$\sigma = c^E \varepsilon - e \Xi, \tag{6}$$

$$D = e \varepsilon + \xi^\sigma \Xi, \tag{7}$$

where  $c^E$  is the elasticity modulus at a constant electric field,  $e$  is the piezoelectric constant, and  $\xi^\sigma$  is the dielectric constant at constant stress, Eqs. (5)–(7) can be substituted into Eq. (4) to give

$$\Pi = \frac{1}{2} \int_{\Omega} c^E (z \cdot w_{,yy})^2 d\Omega + \int_{\Omega} e \Xi z w_{,yy} d\Omega - \frac{1}{2} \int_{\Omega} \xi^\sigma \Xi^2 d\Omega + \frac{1}{2} \int_{\Omega} J J_\alpha \left( \frac{\partial \alpha}{\partial y} \right)^2 d\Omega. \tag{8}$$

#### 4. Applied Loads

The FPSRCB is subjected to aerodynamic and wind loads during the service period. The aerodynamic and wind loads are calculated using the following equations:<sup>(10)</sup>

$$L_a = \frac{1}{2} \rho_a V_\infty^2 S C_L, \tag{9}$$

$$D_a = \frac{1}{2} \rho_a V_\infty^2 S C_D, \tag{10}$$

where  $\rho_a$  is the density of air,  $V_\infty$  is the velocity of the incoming flow,  $S$  is the area of the FPSRCB,  $C_L$  is the lift coefficient, and  $C_D$  is the drag coefficient.  $C_L$  and  $C_D$  are constants. In Ref. 6,

$S = 0.5 \text{ m}^2$ ,  $\rho = 0.414 \text{ kg/m}^3$ ,  $V_\infty = 100 \text{ m/s}$ , and  $C_L$  and  $C_D$  can be computed to be 0.2 and 0.03, respectively, using the simulation result.<sup>(18)</sup>

Equations (9) and (10) can be respectively simplified as

$$L_a = 0.1\rho_a V_\infty^2 b l, \quad (11)$$

$$D_a = 0.015\rho_a V_\infty^2 b l, \quad (12)$$

where  $b$  and  $l$  are the width and length of the FPSRCB, respectively. The joint forces of  $L_a$  and  $D_a$  are denoted as  $F_a$ .

The wind load is<sup>(6)</sup>

$$F_w = \int_0^l q_d c_s C_L \frac{A_w}{V_\infty} \cos(2\pi f_w t) dy, \quad (13)$$

where  $q_d$  is the dynamic pressure,  $c_s$  is the width of the FPSRCB,  $A_w$  is the maximum amplitude of the wind, and  $f_w$  is the frequency of the wind.

Equation (13) can be simplified according to the computation method for the dynamic pressure and lift coefficient.<sup>(2)</sup>

$$q_d = \frac{V_\infty^2}{1600} \cdot 2\pi \quad (14)$$

$$F_w = \frac{3.14 A_w C_L V_\infty l}{800} \cdot b \cdot \cos(2\pi f_w t) \quad (15)$$

The bending of the FPSRCB can be computed as

$$w(y, z) = \frac{(F_w + F_a) l^3}{3E_Y I}, \quad (16)$$

where  $E_Y$  and  $I$  are Young's elastic modulus and the moment of inertia of the FPSRCB, respectively.

The angle of torsion of the FPSRCB can be computed as

$$\alpha(x, y, z) = \frac{F_w + F_a}{2E_Y I} \cdot l^2. \quad (17)$$

$\partial w/\partial x$ ,  $\partial w/\partial y$ ,  $\partial w/\partial z$ ,  $\partial \alpha/\partial x$ ,  $\partial \alpha/\partial y$ ,  $\partial \alpha/\partial z$  and their second-order partial derivatives can be obtained by solving Eqs. (15) and (16).

### 5. Reliability Analysis of FPSRCB

The limit state equation for the reliability computation of the FPSRCB, according to Eqs. (1) and (4), is obtained as

$$G = \Pi - E. \tag{18}$$

In the above equation, by calculating  $G$ , the ratio of the number of  $G > 0$  to the number of operations of  $G$  is determined to be the reliability of the FPSRCB.

Equation (18) can be simplified as follows by using Eqs. (2), (3), (9), and (16).

$$2G = \int_{\Omega} c^E z^2 (A_1 E)^2 + 2e\Xi z (A_1 E)^2 + IJ_{\alpha} (A_2 E)^2 d\Omega + \xi^{\sigma} \Xi^2 S_p - \rho \int_{\Omega} A_1^2 \left[ z^2 B^2 + (C + D)^2 + z^2 A_2^2 (C + D)^2 \right] d\Omega, \tag{19}$$

where  $A_1 = \frac{l^3}{3E_Y I}$ ,  $A_2 = \frac{l^2}{2E_Y I}$ ,  $B = \frac{\partial F_w}{\partial y} + \frac{\partial F_a}{\partial y}$ ,  $C = \frac{\partial F_w}{\partial y} \frac{dy}{dt} + \frac{\partial F_a}{\partial y} \frac{dy}{dt}$ ,  $D = \frac{\partial F_w}{\partial z} \frac{dz}{dt} + \frac{\partial F_a}{\partial z} \frac{dz}{dt}$ ,  $E = \frac{\partial^2 F_w}{\partial y^2} + \frac{\partial^2 F_a}{\partial y^2}$ .

The parameters of the FPSRCB are shown in Table 1 with their coefficient of variation of 0.005.<sup>(6)</sup>

In Table 1,  $l_p$ ,  $h_p$ , and  $b_p$  are the length, thickness, and width of the piezoelectric actuator, respectively. Two piezoelectric actuators are pasted on the FPSRCB along the length of the cantilever beam. The material of the FRCB is aluminum 2024-T3, the material of the piezoelectric actuator is lead zirconate titanate, and the material of the piezoelectric sensor is polyvinylidene fluoride.

The deflection of the FRCB is obtained by using Eq. (16).

$$w(y, z) = 5.91 \times 10^{-4} V_{\infty}^2 + 2.8 \times 10^{-4} V_{\infty} \cos(2\pi f_w t) \tag{20}$$

Table 1  
Parameters of the FPSRCB and their mean values.

| Parameter       | Value                                   | Parameter      | Value                   |
|-----------------|---|----------------|-------------------------|
| $L$             | $350 \times 10^{-3}$ m                  | $V_{\infty 1}$ | 5 m/s                   |
| $H$             | $1 \times 10^{-3}$ m                    | $V_{\infty 2}$ | 7.5 m/s                 |
| $B$             | $40 \times 10^{-3}$ m                   | $f_{w1}$       | 1 Hz                    |
| $E$             | 73.1 GPa                                | $f_{w2}$       | 2 Hz                    |
| $I$             | $2 \times 10^{-12}$ m <sup>4</sup>      | $l_p$          | $45.9 \times 10^{-3}$ m |
| $\rho$          | 2780 kg/m <sup>3</sup>                  | $h_p$          | $0.25 \times 10^{-3}$ m |
| $e$             | 12 N/Vm                                 | $b_p$          | $20.6 \times 10^{-3}$ m |
| $\xi^{\sigma}$  | $5.92 \times 10^{-9}$ CV/m <sup>2</sup> | $c^E$          | 67 GPa                  |
| $\rho_{\alpha}$ | 0.414 kg/m <sup>3</sup>                 | $\rho_p$       | 770 kg/m <sup>3</sup>   |

Its changes in 10 s are shown in Fig. 4.

The torsional angle of the FRCB is obtained by using Eq. (17).

$$\alpha(x, y, z) = 1.38 \times 10^{-3} V_{\infty}^2 + 6.54 \times 10^{-4} V_{\infty} \cos(2\pi f_w t) \quad (21)$$

Its changes in 10 s are shown in Fig. 5.

It can be seen from Figs. 4 and 5 that the deflection and torsional angle of the FRCB change repeatedly under aerodynamic and gust loads, causing the FRCB to flutter rapidly, under the following conditions: a wind speed of  $V_{\infty 2}$  and a wind frequency of  $f_{w1}$  in Table 1;<sup>(6)</sup> to one piezoelectric actuator, a voltage of 0–220 V is applied, reducing 20% of the maximum vibration amplitude of the FPSRCB; and to two piezoelectric actuators, a voltage of 0–220 V is applied, reducing 43% of the maximum vibration amplitude, where the maximum vibration amplitude is normalized to 1 mm.

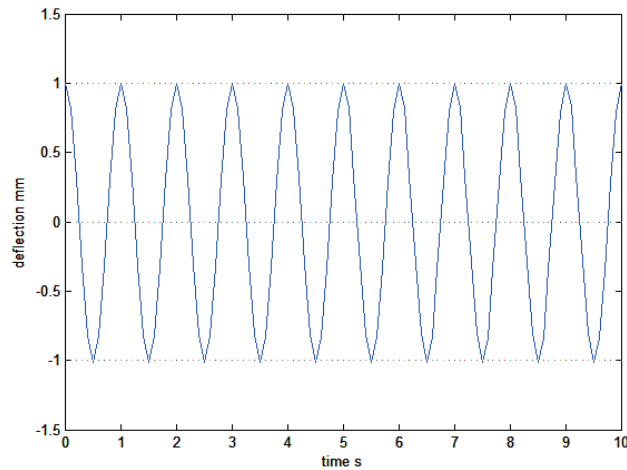


Fig. 4. (Color online) Variation in the deflection of the FRCB.

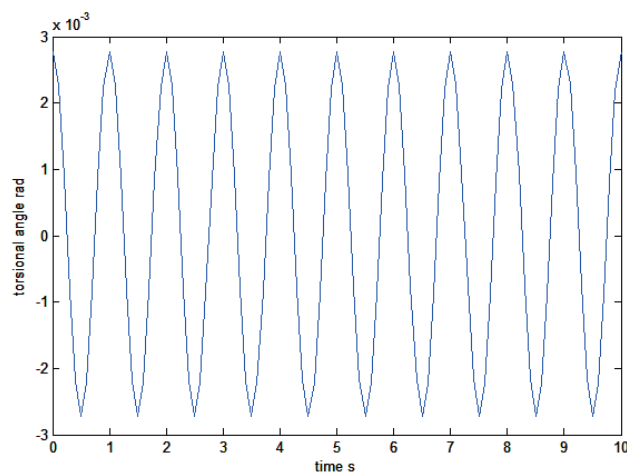


Fig. 5. (Color online) Variation in the torsional angle of the FRCB.



Table 2  
Reliability of the FPSRCB.

| Parameter   | Actuator 1 | Actuator 2 |
|-------------|------------|------------|
| $V_w$ (m/s) | 7.5        | 7.5        |
| $f_w$ (Hz)  | 2          | 2          |
| Times       | $10^5$     | $10^5$     |
| Reliability | 0.9999     | 0.9998     |

On the basis of the data in Table 1 and the parameters in Ref. 5, Eq. (18) is applied  $10^5$  times in the simulation, which is based on the design standards in Ref. 3 by using Matlab software according to the Monte Carlo method. In structural reliability analysis, the Monte Carlo method is used to accurately compute the failure probability. The parameters in Table 1 are generated from  $10^5$  data by using the random numbers method when the coefficient of variation is 0.005. Each parameter is taken as one data at random intervals at a time, and the data of 18 parameters are used at a time in the computation.  $10^5$  data are obtained in total. Then, a value greater than 0 is the reliability compared with the total number of samples. The random data will be substituted into Eqs. (19) and (20) to produce  $10^5$  random data. Equation (19) is applied a total of  $10^5$  times in the simulation.

The value of  $w$  in  $E_b$  and  $E_t$  is assigned to 1 mm in Ref. 6, one actuator can be used to reduce the vibration by 20%, and two actuators can be used to reduce the vibration by 43%. For conservatism, the value of  $w$  in  $\Pi$  is assigned to 0.8 mm when using one actuator and 0.57 mm when using two actuators in this study. The first actuator is 15 mm from the base of the beam, whereas the second actuator is 10 mm from the first. The two actuators are of the same size, right in the middle of the beam width. With the computations conducted  $10^5$  times in simulations, the results are shown in Table 2.

It can be seen from Table 2 that when one actuator is used to reduce the vibration amplitude of the FPSRCB, the reliability is 0.9999, and when two actuators are used to reduce the amplitude, the reliability is 0.9998. This result shows that the design of the FPSRCB is feasible. It can be seen from Table 2 that the reliability of the FPSRCB of two actuators is lower than that in the presence of one actuator, because the two actuators are in parallel and the actuator is at risk of breakdown under excitation voltage. It has been shown that the simulation results of the proposed method are compatible with the results in Ref. 18, indicating the feasibility of the proposed method. The proposed method has also been verified using the results of the wind tunnel experiment reported in Ref. 5.

## 6. Conclusions

In this study, the problem of reliability associated with the flutter of the FPSRCB under complex wing loads could be effectively alleviated by using piezoelectric actuators. The external loads of the FPSRCB detected by the piezoelectric sensors were computed, and the dynamic motion and deformation mode of the FPSRCB were analyzed. According to the given parameters, the reliability of the FPSRCB, in which the flutter is reduced by using one and two actuators, is simulated, and the results are consistent with those in the literature. The reliability calculation

model for the FPSRCB presented in this paper has practical engineering significance and feasible applications to the reliability design and maintenance of UAV wings, wind turbine devices, micromachines, and others.

### Acknowledgments

The work described in this paper was supported in part by the Ningxia Key Research and Development Program, China (2022BSB03101), the Ningxia Fundamental Research Project (2023A1955), and the High-level Talent Project of Ningxia Normal University.

### References

- 1 S. Sikdar, S. K. Singh, P. Malinowski, and W. Ostachowicz: *J. Intell. Mater. Syst. Struct.* **33** (2021) 1487. <https://doi.org/10.1177/1045389X211057225>
- 2 N. Luo, H. Liao, and M. Li: *Wind Struct.* **25** (2017) 493. <https://doi.org/10.12989/was.2017.25.5.493>
- 3 C. L. Pan, J. L. Rong, T. F. Xu, and D. L. Xiang: *J. Astronaut.* **42** (2021) 881. <https://doi.org/10.3873/j.issn.1000-1328.2021.07.008>
- 4 Y. F. Fang, K. F. Tee, and L. Wen: *Sens. Mater.* **33** (2021) 2407. <https://doi.org/10.18494/SAM.2021.3210>
- 5 M. A. Neto, W. Yu, and S. Roy: *Finite Elem. Anal. Des.* **45** (2009) 295. <https://doi.org/10.1016/j.finel.2008.10.010>
- 6 T. de S. S. Versiani, F. J. Silvestre, A. B. Guimarães Neto, D. A. Rade, R. G. A. da Silva, M. V. Donadon, R. M. Bertolin, and G. C. Silva: *Aerosp. Sci. Technol.* **86** (2019) 762. <https://doi.org/10.1016/j.ast.2019.01.058>
- 7 Q. Zhang, S. Jia, J. Chen, Y. Xu, and Z. Yu, C. Cai, and Y. Pan: *J. Thu. (Sci & Technol)* **62** (2022) 423. <http://jst.tsinghuajournals.com/CN/Y2023/V63/I3/423>
- 8 Bilal El Yousfi, Abdenour Soualhi, Kamal Medjaher, and François Guillet: *Mech. Syst. Signal. Pr.* **166** (2022) 108435. <https://doi.org/10.1016/j.ymssp.2021.108435>
- 9 G. Quattrocchi, A. Iacono, P. C. Berri, M. D. L. D. Vedova, and P. Maggiore: *Actuators* **10** (2021) 194. <https://doi.org/10.3390/act10080194>
- 10 X. Zhang, R. Wang, Z. Wang, S. Zhang, X. Qin, and X. Tan: *J. NWPU* **35** (2017) 661. <https://journals.nwpu.edu.cn/xbgdydxb/CN/abstract/abstract6815.shtml>
- 11 N. Tsushima and W. Su: *Aerosp. Sci. Technol.* **79** (2018) 297. <https://doi.org/10.1016/j.ast.2018.05.056>
- 12 S. Petroni, G. Maruccio, F. Guido, M. Amato, A. Campa, A. Passaseo, M. T. Todaro, and M. De Vittorio: *Microelectron. Eng.* **98** (2012) 603. <https://doi.org/10.1016/j.mee.2012.05.055>
- 13 H. Nawaz, M. U. Masood, M. M. Saleem, J. Iqbal, and M. Zubair: *Microelectron. Reliab.* **104** (2020) 113544. <https://doi.org/10.1016/j.microrel.2019.113544>
- 14 D. J. Jerez, H. A. Jensen, and M. Beer: *Mech. Syst. Signal Process.* **166** (2022) 108397. <https://doi.org/10.1016/j.ymssp.2021.108397>
- 15 Y. Fang, K. F. Tee, Z. Cheng, and Y. Xu: *Math. Probl. Eng.* **2021** (2021) 5713902. <https://doi.org/10.1155/2021/5713902>
- 16 S. S. Ahmad, L. Tom, A. L. Rocca, S. L. Rocca, G. Vakil, C. Gerada, and M. Benarous: *Energies* **15** (2022) 15041467. <https://doi.org/10.3390/en15041467>
- 17 A. Antoniadis, S. Lambert-Lacroix, and J.-M. Poggide: *Reliab. Eng. Syst. Safe.* **206** (2022) 107312. <https://doi.org/10.1016/j.res.2020.107312>
- 18 B. Yu, S. Si, J. Lin, and X. Jing: *Mach. Design Manuf.* **337** (2019) 135. <https://doi.org/10.19356/j.cnki.1001-3997.2019.03.034>

## About the Authors



**Fang Yongfeng** received his B.S. degree from Northwest Normal University, China, in 2000, and his M.S. and Ph.D. degrees from Xidian University, China, in 2008 and 2013, respectively. From 2008 to 2010, he was an assistant professor at Longdong University, China. Since 2013, he has been a professor at Guizhou University of Science Engineering. He is working at Ningxia Normal University. His research interests are in the reliability of sensors. ([fangyf\\_9707@126.com](mailto:fangyf_9707@126.com))



**Zizhe Fang** received his B.S. degree from Northeastern University, China, in 2021, and he is pursuing his master's degree at Northeastern University from 2021. His research interests are in the optimal design of robot systems. ([501345357@qq.com](mailto:501345357@qq.com))



**Kong Fah Tee**, B.Eng. (Hons) Ph.D. PGCert. (HE) MBA DIC FHEA is an associate professor at King Fahd University of Petroleum and Minerals. He was previously a professor at INTI International University and a reader at the University of Greenwich. He focused his research effort on structural system identification and health monitoring, structural reliability and failure analysis, applications of artificial intelligence, experimental stress analysis, fatigue, fracture mechanics, and structural dynamics. ([kftee2010@gmail.com](mailto:kftee2010@gmail.com))



**Tuo Yaofei** received his B.S. degree from Northwestern Poly-Technique University, China, in 1992, and his M.S. and Ph.D. degrees from Xidian University, China, in 2004 and 2007, respectively. From 2008 to 2016, he was an assistant professor at Yulin University, China. Since 2017, he has been a professor at Yulin University. His research interests are in the reliability and optimal design of mechanical systems. ([tuoyf-2008@163.com](mailto:tuoyf-2008@163.com))